The effect of prestrain on low and high temperature creep in Ti834

Mark Whittaker[1], Paul Jones[1], Cameron Pleydell-Pearce[1], David Rugg[2], Steve Williams[2]

[1] University of Wales Swansea, Singleton Park, Swansea. SA2 8PP

[2] Rolls-Royce plc, Moor Lane, Derby. DE24 8BJ

Abstract

The low and high temperature creep properties of the α+β titanium alloy Ti834 have been studied for various levels of applied plastic prestrain. Evidence is shown that the prestrain at room temperature causes the formation of quasi-cleavage facets in a manner described by the Evans-Bache model. These facets are also produced when the material is creep tested at room temperature, although larger areas of faceting are found. The applied prestrain causes a drop in the strain at failure at room temperature due to a high dislocation density inhibiting further movement of dislocations. At high temperature this increase in applied prestrain results in an accelerated creep rate. This is attributed to a number of issues, including increased thermal energy allowing greater dislocation recovery and mobility. Swaged Ti834 material is also considered and is shown to behave similarly to highly prestrained material with evidence of strain hardening and reduced cold creep rate.

Keywords: Prestrain, Titanium, Facets, Creep

Introduction

The near alpha titanium alloy Ti834 was developed for high temperature applications and shows exceptional mechanical properties up to 630°C. This fact, accompanied by the desirable strength to weight ratio for titanium alloys, has made Ti834 a popular choice with designers of gas turbines for compressor disc and blade applications.

To achieve an optimum compromise between high temperature creep and lower temperature fatigue, careful control of the microstructure has been applied by alloy developers. However, previous work[1] has shown that Ti834 is one of a series of near α and α+β titanium alloys which show a sensitivity to dwell periods at low temperature, loosely termed 'cold creep'. This type of failure was first appreciated in service during the early 1970s when two uncontained fan disc failures were shown to be as a result of dwell fatigue in the near α alloy Ti685.

Subsequent research[2] has shown that this type of dwell sensitivity is related to the formation of 'quasi-cleavage' facets that often occur subsurface and lead to crack initiation, promoting premature failure. The Evans-Bache model seeks to describe the formation of initial facets in terms of dislocation pile ups at interfaces between hard and soft grains, or possibly even structural units. These facets, which generally have a near basal plane orientation, develop due to the gradual separation of intense slip bands under the action of a tensile stress normal to the slip plane. The presence of strong and weak regions within the microstructure facilitates this mechanism through stress redistribution. Grains that have a basal plane orientation nearly perpendicular to the loading direction act as a 'strong' grain, i.e. slip is difficult. However, if adjacent grains have easily available slip systems, they can provide the mechanism for dislocation pile ups at the boundary. The pile up provides the required induced shear (τ_f) and tensile (σ) stress on the unfavourably orientated basal plane with τ_s the resolved shear stress on the 'weak' grain, Figure 1. More recent research has established that the angle at which these facets form is a function of loading condition[3].

Although the model aptly describes the process of facet generation, which has more recently been extended[4,5] and supported with experimental evidence in the near alpha titanium alloy Ti685[6], the macroscopic loading conditions under which extensive facet formation occurs have not been so well described. In particular the formation of facets under application of a constant load (or stress) in a conventional creep test is an area of interest.

Furthermore, it is widely acknowledged that the application of prestrain at room temperature can produce marked alterations in the creep rate of titanium alloys[7]. However, the current work seeks to

investigate how these creep rates and other mechanical properties are affected by the presence of quasi-cleavage facets which may be introduced through prestrain.

The paper seeks to address these issues through a series of different loading conditions. Ti834 material was supplied in an as received condition from a disc forging, although orientation was not recorded. These specimens were then prestrained to four different levels, 2% compressive prestrain (referred to as -2%), 2% tensile prestrain, 8% tensile prestrain while a batch of specimens remained in the as received condition (referred to as 0%). The prestraining was used to simulate prior working operations on the material. Specimens were subsequently tested under hot and cold creep conditions along with stress relaxation and fatigue tests, with SEM analysis used to explore fracture surface features including facet formation.

Experimental method

The Ti834 was found to have a bimodal microstructure with primary alpha grains with a semi-major axis ranging from 20-200μm in diameter, and grains encompassing transformed product with a semi-major axis ranging from 50-200μm in diameter. The crystallographic texture of the material was essentially random, which limited concerns about specimen orientation previously mentioned, Figure 2.

Prestraining was performed on a Mayes servo hydraulic test machine, under strain control, using an axial MTS extensometer with a gauge length of 12mm. Specimens were loaded to strains of -2%, 2% or 8% using a constant strain rate of 0.5%/sec. They were then unloaded to zero load and removed from the test machine prior to subsequent testing. The average modulus on loading into tension or compression was found to be 120GPa, consistent with published values[8].

Specimens from each prestrain batch were then tested under one of the following conditions:-

i) Ambient temperature (20ºC) creep testing at 950MPa and under constant load conditions.

ii) High temperature creep testing (600°C) at 400MPa and under constant load conditions.

iii) Strain control fatigue under R=-1 conditions at a constant strain rate of 0.5%/sec until failure (Classed as a 10% drop in load from the stabilised condition) using a trapezoidal 1-1-1-1 waveform, according to BS7270[9].

iv) Stress relaxation for 3 hours at a constant strain of 1%. These specimens were then cycled to failure under the same conditions used in (iii).

Results

Although the applied prestrains have been quoted as -2%, 2% and 8%, the amount of residual plastic prestrain is considerably less in each case. Assuming the material unloads elastically at the end of pre-straining, the residual plastic strain in each case is approximately -1.25%, 1.25% and 7.25%. Although data is available for the effect of prestrain on both the fatigue and creep properties of titanium alloys[7,10], these are mainly based on significantly smaller levels of prestrain than have been considered in this case.

Figure 3 shows the stress-strain characteristics of the material during the application of the 2% and -2% prestrains. It is clear that the yield stress is higher in compression than in tension.

Figure 4 compares creep curves at 20°C. The strains do not include strain on loading, which differed significantly for the four levels of prestrain. Figure 5 shows these loading curves and it is clear that the 2% prestrain and particularly the 8% prestrain specimens strain harden significantly. Because of prior loading in compression, the -2% specimen displays a decrease in yield stress.

It is clear from Figure 4 that prestraining causes a reduction in the strain at failure, at all levels of prestrain. It is also noticeable that a significant reduction in the amount of primary creep occurs in the prestrained specimens. The 8% prestrain specimen shows only a small amount of primary creep and essentially no secondary creep. This specimen was removed, unfailed, after ten days with little evidence of creep.

In all cases there is little or no evidence of tertiary creep. This is a consequence of the low temperature testing and the fact that tests were conducted under constant load rather than constant stress.

Figure 6 summarizes creep at 600°C and a constant load. All specimens show a more substantial tertiary creep phase than was seen at 20°C.

Significant differences are now clear between the data at 20°C and 600°C. Perhaps the most easily recognisable is the fact that the 8% prestrain specimen, which showed essentially no creep at 20°C now shows the fastest rate, lowest strain at fracture and shortest time to fracture of all the specimens.

The 2% and -2% curves are quite similar although the onset of tertiary creep is earlier in the 2% specimen. A clear trend observed is that at this temperature an increase in prestrain leads to a decrease in strain at fracture and time to fracture.

Discussion

In order to evaluate the effect of different loading conditions on facet formation, it is first necessary to isolate conditions where facet formation is not promoted. In the current work, fatigue testing of as

received (0% prestrain) specimens showed little evidence of facetting across the specimen. This is to be expected under fully reversed strain control loading conditions, since the mean stress on the specimen will be low and the reversible nature of the applied stress means that dislocation build-ups are easily relieved. This provides a control condition, allowing for the isolation of the effects of prestraining and stress relaxation on the fractographic features within these specimens.

The application of prestrain to specimens initially appeared to be a facet-forming process, with isolated facets being observed in both 2% and -2% test specimens, which were subsequently cycled to failure under the strain control conditions described above. Furthermore, more extensive facetting was observed in the 8% prestrain specimen, Figure 7. Previous work however[11] has indicated that facet formation during monotonic loading is unlikely. Instead, when a period of stress relaxation is introduced, the time dependent nature of the process means that facets form more readily. On closer inspection of Figure 3(a) this has significant bearing on the current work. A small delay occurred between peak strain being achieved and unloading of the specimen to zero load. Although this delay constituted only a few seconds, it is evident from the drop in stress at the end of the loading curve that significant stress relaxation has occurred. This is more likely to be the source of facet formation in these tests. At 8% prestrain, significantly more dislocations have been generated, and as such more facets form due to pile ups at grain boundaries.

The results from figure 4 for creep tests at room temperature can be interpreted by considering the generation of dislocations through plastic deformation brought about by prestraining at room temperature. The presence of these dislocations can be inferred from the strain hardening effect seen in the 2% and 8% prestrain specimens on loading, Figure 5. It is interesting first to note that a decaying primary phase is observed in each test, which is followed in the 0%, 2% and -2% tests by a short tertiary phase before final failure. The 8% prestrain test was removed from test after ten days because of its extremely slow strain rate. Figure 8 illustrates that apart from a significant decrease in the 8% test, the prestrain had little effect on creep strain rate. It is clear, however, that the prestrain had a significant effect on the strain at failure, with significant reductions in the 2% and -2% tests. The dislocations generated by the prestrain process restrict further dislocation movement and final failure occurs at greatly reduced strains as necking occurs. The extremely high dislocation density generated by 8% prestrain is such that almost all dislocation movement is difficult, and the strain rate falls dramatically.

The fracture surfaces of creep specimens showed extensive areas of quasi-cleavage faceting providing evidence that dislocation creep facilitates this facet formation, Figure 9. Previous research into this alloy[12] has shown evidence of macrozone formation (large areas of common crystallographic orientation) that may be related to the cold dwell effects that are often evident under fatigue testing. EBSD analysis of the section studied however has not shown any evidence of such macrozones, Figure

10. It can be seen that there is little ordered texture over lengths greater than approximately 200μm. It is acknowledged that the individual quasi-cleavage facets making up the larger faceted areas seen in the low temperature creep tests correlates well with areas of common orientation shown in the crystallographic orientation map, and therefore it is likely that these faceted areas are of a common orientation. It is also interesting to note that these areas show approximately the same dimensions as the grains of transformed product or primary alpha grains seen in the microstructure.

It is interesting to consider, however, the stress relaxation tests performed as part of the programme of work. Since the mechanisms involved in stress relaxation will be similar to the strain accumulation evident in the cold creep tests, it is expected that similar fractographic features would be evident. In fact, the cleavage facets that are produced show distinct differences to those produced in the creep specimens. Rather than the large areas of facetting in the creep specimens, facet areas are now small and isolated from each other, with facets seeming to be related to primary alpha grains which have previously been reported to have basal or near basal orientations[3].

To illustrate the reason for the larger facetted areas in the creep specimen, it is useful to consider the accumulation of plastic strain during a stress relaxation test

$$\varepsilon = \varepsilon_{el} + \varepsilon_{pl}$$

$$\varepsilon = \left(\varepsilon_{el} - \frac{\Delta\sigma}{E} \right) + \varepsilon_{pl} + \Delta\varepsilon_{pl}$$

And clearly a fixed total plastic strain is exchanged for elastic strain in the form

$$\Delta\varepsilon_{pl} = \frac{\Delta\sigma}{E}$$

Typical values of $\Delta\sigma$ are 100→150MPa giving

$$\Delta\varepsilon_p = 0.00083 \rightarrow 0.00125 = (0.083 \rightarrow 0.125)\%$$

And comparing these values to the levels of plasticity seen in the creep tests, Figure 4, it becomes clear that the significantly lower levels of plastic strain accumulated in the stress relaxation tests limit the number of facets produced.

As described earlier, it is stress relaxation of this type, at the end of the prestrain period which generates facets, rather than the prestrain loading itself. Figure 11 shows the stress relaxation characteristics of the four different prestrain levels. The vertical axis is plotted as normalized stress, i.e. stress divided by the peak stress reached during loading. This gives a clearer indication of the processes occurring during the period of relaxation, by removing the issues of strain hardening (2% and 8% prestrain) or reverse Baushinger effect (-2% prestrain) which cause the tests to reach various peak stresses[13]. Similar trends

are seen to the room temperature creep tests, in that for the lower amounts of prestrain, little variation is seen to the as received material. However, for the 8% prestrain specimen, the high dislocation density again prohibits the movement of further dislocations, and as such little stress relaxation is seen.

At 600°C significantly different results are found in creep tests to those performed at room temperature, Figure 6. Clearly, increased prestrain now results in an increase in creep strain rate and a decrease in time to rupture and strain at rupture. At these temperatures in Ti834, due to the increase in thermal energy, dislocations are far more mobile and processes such as climb and cross slip are promoted, resulting in a higher creep strain rate and hence reduced rupture time. It is clear that the mechanisms operating at low temperature are quite different to those at high temperature, a view reinforced by the now prolonged tertiary period of deformation in each specimen and extensive void formation at 600°C.

Swaged material

To explore extreme pre-straining a batch of the Ti834 underwent swaging in which the bar was elongated by 108%. Figure 12 shows the microstructure and texture of the material. All tested specimens were aligned with the direction of extrusion of the swaged bar.

The swaging process has clearly had a marked effect on the material. The vertical axis of the micrograph is parallel to the direction of elongation. It is clear that the primary alpha grains have experienced considerable deformation in this direction. The crystallographic texture of the material has also been severely affected. The as received material showed a very weak texture but that has now been replaced by a well defined fibre texture. The (0001) basal pole figure is taken from the end of the cylindrical bar and shows that basal planes lie in a fan shaped distribution, approximately parallel to the length of the bar. This is consistent with other work[14]. Clearly such a dramatic change in structure impacts on the mechanical properties and this was evident from two tensile tests. A dramatic drop in the modulus value was found with the swaged material having a value of approximately 100GPa, compared with 120GPa for the as received material. The change in the modulus is a consequence of the strong texture of the material. Previous work[15] has shown that basal plane orientation can cause differences in the modulus by as much as ±20GPa and this is the case here with loading near parallel to the majority of basal planes.

Also clear was a significant increase in the UTS of the material, from 1100MPa in the as received material to approximately 1350MPa in the swaged material. This increase is a consequence of the large dislocation density induced and associated with strain hardening.

The resultant high dislocation density led to an even slower creep rate than in the 8% prestrain specimen. However, the material was heat treated to investigate any evidence of recovery. Figure 13

shows the creep curves of the swaged material following heat treatments of 2 hours at 450°C, 600°C and 700°C respectively. The curve for the 0% prestrain material is included for comparison purposes. Following the 450°C and 600°C treatments the creep rate is still essentially zero. At 700°C there is a slight increase in the creep rate, particularly during primary creep. This suggests that at this temperature a certain amount of recovery is occurring. It is likely that had the time of the heat treatments been increased, further increases in the creep rate would have been seen as the level of recovery increased. Indeed when the swaged material was creep tested at 600°C, Figure 14, it shows a faster creep rate than any of the prestrained specimens, indicating that dislocation recovery at prolonged periods at high temperature is playing a major role. A number of other factors may influence the creep rate at this temperature. Dynamic recrystallisation is a possibility under these conditions and may cause microstructural variations that increase creep rate. It is clear that extensive ductile void formation, Figure 15, occurs at this temperature and is probably a consequence of enhanced dislocation mobility. The voids will certainly accentuate the onset of tertiary creep. Furthermore, facets formed at 20°C during the prestrain process will still exist in the material and will increase the rate of strain accumulation. These combined factors lead to a situation where an increase in prestrain clearly leads to a faster rate and reduced time to failure.

Modelling creep curves

Traditionally it has been shown that the shape of high temperature creep curves can be accurately described using the theta projection method[16]. Previous research has shown that titanium alloys are no exception to this[17]. However as temperatures drop below $0.4T_m$, the characteristics of these alloys change, although there is still significant strain accumulation under applied load. At these lower temperatures the creep curve takes a distinctly different shape, and a different method of describing the curve is necessary. Figure 16 illustrates the room temperature creep curve in Ti834. A numerical description of the curve has been achieved by summing a logarithmic strain relationship with a linear damage criterion, $\varepsilon_t = \alpha_1 \log(\alpha_2 t+1) + \alpha_3 t$. The second term defines linear damage and represents the formation of facets within the material. Linear damage implies a constant rate of damage accumulation. A constant damage rate is associated with an exponential failure criterion. Such a criterion can be derived from a ‘weak link’ theoretical model. In the present case, the weak link can be associated with critical regions within the microstructure. Perhaps the most interesting observation is that the numerical description requires that facet formation begins at the beginning of the creep test, and continues through to final failure.

Conclusions

- Stress relaxation or creep at room temperature causes the formation of quasi-cleavage facets through dislocation piles ups at the boundaries of suitably orientated grains. Creep leads to larger faceted areas.
- Significant prestrain leads to a reduction in creep rate at room temperature as dislocation stress fields inhibit the movement of further dislocations.
- At higher temperatures the increased availability of mechanisms such as cross slip and climb mean that dislocation movement occurs more easily and increased levels of prestrain lead to an increase in creep rate but lower strain at failure.
- Swaged material behaves in a similar manner to heavily prestrained material. However, material deformation through this process can significantly alter material behaviour, and processes such as texture development and strain hardening require consideration for mechanical properties evaluation.
- As an alternative to use of the theta method at high temperature, low temperature creep in titanium alloys can be modeled using a logarithmic strain approach summed with a linear damage criterion.

Acknowledgements

The authors would like to thank Rolls-Royce plc for their help and input during the course of this work.

References

[1] M.R. Bache, M. Cope, H.M. Davies, W.J. Evans and G. Harrison, “Dwell sensitive fatigue in a near alpha titanium alloy at ambient temperature”, Int. J. Fatigue, 19, Supp. 1, 1997, pp. S83-S88.

[2] W.J. Evans, M.R. Bache “Dwell and environmental aspects of fatigue in α/β titanium alloys, in Fatigue Behaviour of Titanium Alloys, Eds. R.R. Boyer, D. Eylon and G. Lutjering, TMMS, Warrendale, pp. 99-110, 1999.

[3] V. Sinha, M.J. Mills, J.C. Williams, “Crystallography of fracture facets in a near alpha titanium alloy”, Metallurgical and Materials Transactions A, Vol. 37A, June 2006, pp2015-2026

[4] V. Hasija, S. Ghosh, M.J. Mills, D.S. Joseph “Deformation and creep modelling in polycrystalline Ti-6Al alloys”, Acta Materialia, 51, 2003 pp 4533-4549

[5] F.P.E. Dunne, D. Rugg, A. Walker "Lengthscale-dependent, elastically anisotropic, physically-based hcp crystal plasticity: Application to cold-dwell fatigue in Ti alloys", Int. Journal of Plasticity, 23, 2007, pp 1061-1083

[6] E.E. Sackett, L. Germain and M.R. Bache; "Crystal plasticity, fatigue crack initiation and fatigue performance of advanced titanium alloys", Int. J. Fatigue, 29(9-11), 2007, pp. 2015-2021.

[7] B.C Odegard, A.W. Thompson "Low temperature creep of Ti-6Al-4V", Metallurgical and Materials Transactions B, Vol. 5 No.5, 1973, pp 1207-1213

[8] Timet website, www.timet.com

[9] BS7270, "British standard method for constant amplitude strain controlled fatigue testing", British Standards Institution, 1990

[10] DB Lanning, T Nicholas, GK Haritos "Effect of plastic prestrain on high cycle fatigue of Ti-6Al-4V", Mechanics of Materials 34, 2002, pp127-134

[11] W.J. Evans, "Optimising mechanical properties in alpha + beta titanium alloys" Materials Science and Engineering A243 (1998) pp 89-96

[12] L. Germain, M. Bache "Crystallographic texture and the definition of effective structural unit size in titanium products" Proceedings of the 11th International conference on Titanium, Kyoto 2007, pp 953-956

[13] M.T. Whittaker, W.J. Evans, "Effect of prestrain on the fatigue properties of Ti834", International Journal of Fatigue, Vol. 31, Iss. 11-12, 2009, pp 1751-1757

[14] G. Lutjering, "Influence of processing on microstructures and mechanical properties of $\alpha+\beta$ Titanium alloys", Material Sci & Eng A243 (1998) pp 32-45

[15] A.W. Bowen, "Texture stability in heat treated Ti6-4 alloys", Material Sci & Eng Vol. 29, 1977, pp 19-28

[16] W. Harrison, W.J. Evans, "Application of the Theta projection method to creep modelling using Abaqus", 2007 UK ABAQUS users regional meeting.

[17] A.R. Ward, "Creep and creep fracture of the alpha and beta titanium alloy 6246", PhD Thesis, University of Wales Swansea, 2002

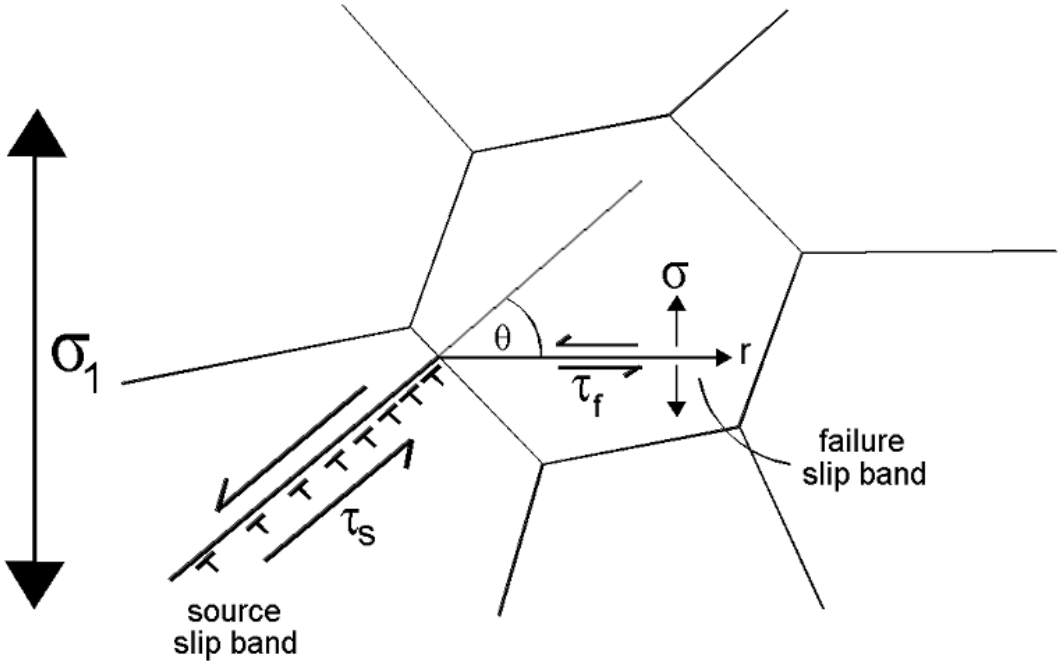

Figure 1: Dislocation pile ups at grain boundaries induce a combination of shear and tensile stresses which allow facet formation in titanium alloys, usually with a basal or near basal plane orientation.

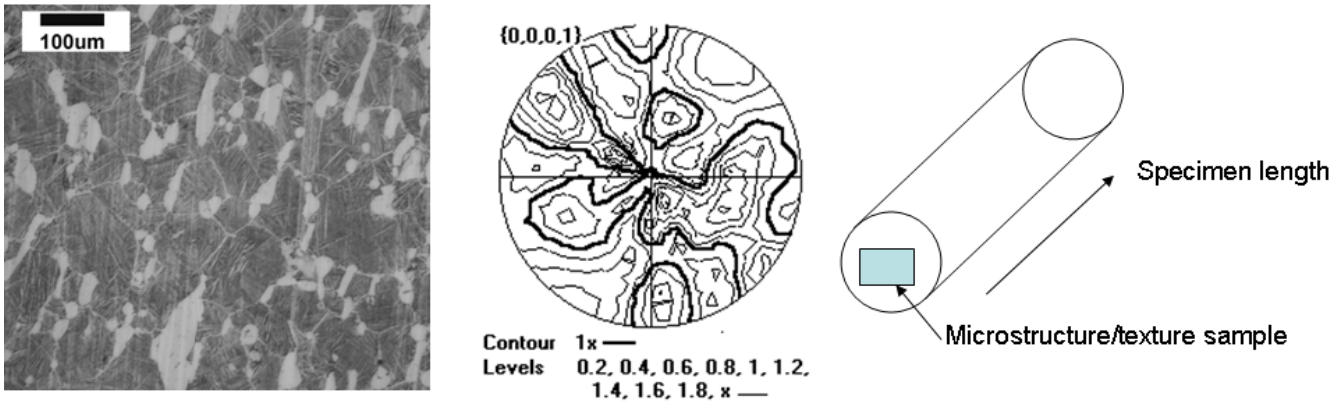

Figure 2: Microstructure and texture of Ti834. A mixture of equiaxed and slightly elongated primary alpha grains with a maximum diameter of 200µm are evident. The crystallographic texture is of a transformation type with low intensity. Samples were also taken for microstructure and texture analysis orthogonal to that shown, with no significant differences evident. (Texture maps produced over an area of 0.5 x 0.5mm)

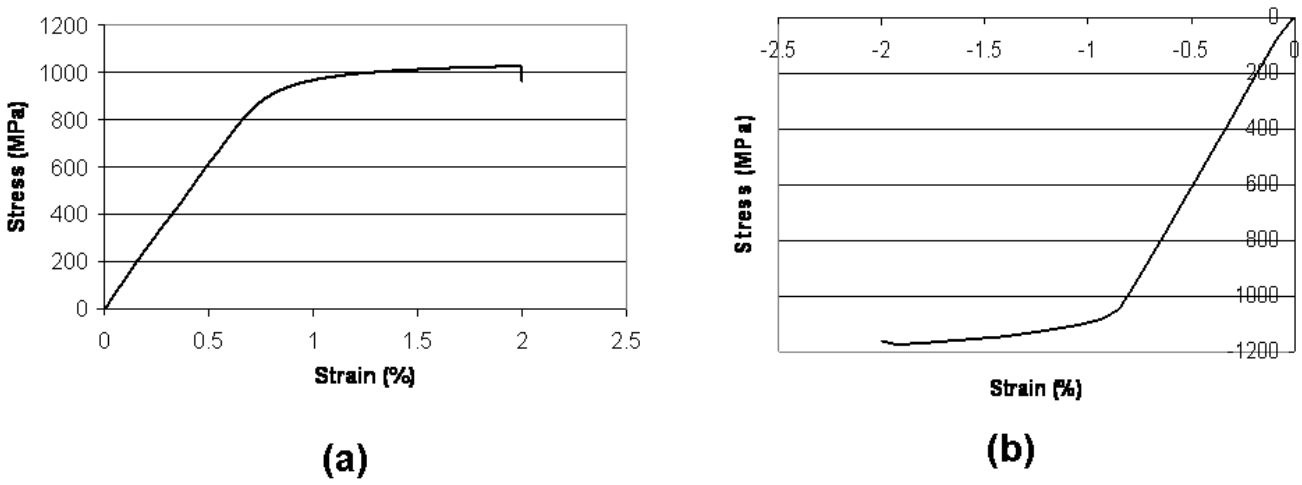

Figure 3. Loading curves for prestrain of a) 2% b) -2%. A slightly higher yield stress can be observed in compression.

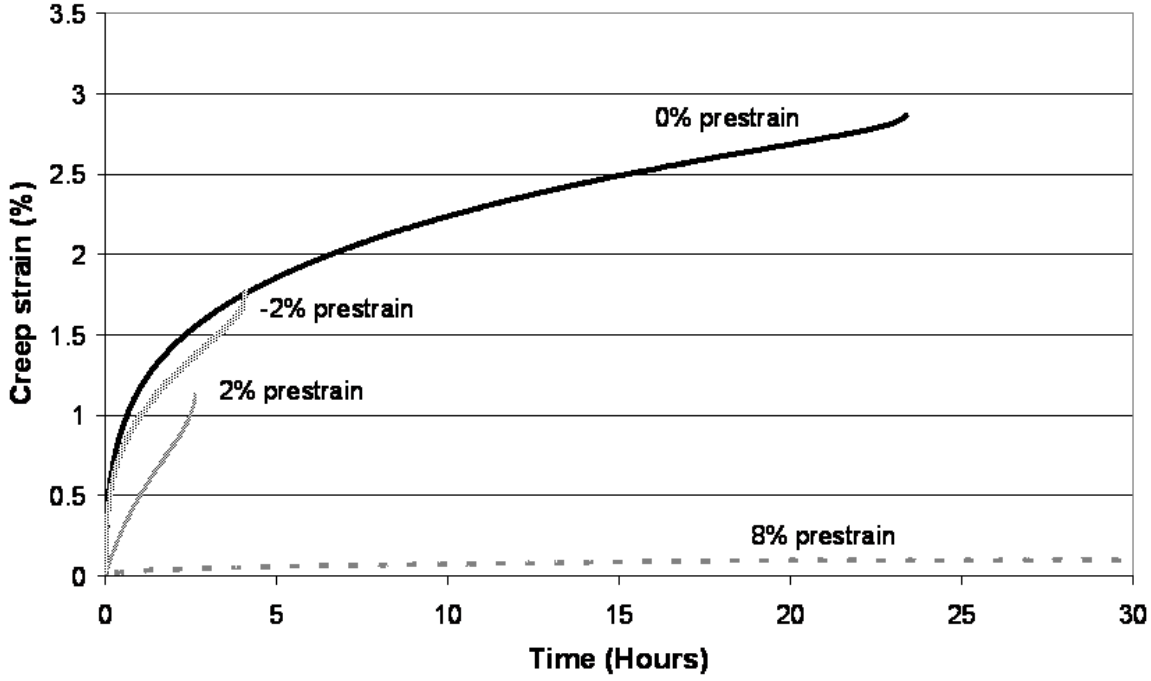

Figure 4: Creep curves at 20°C at a stress of 950MPa. Increases in prestrain cause a reduction in strain at failure, and it can be seen that the high dislocation density in the 8% prestrain specimen results in a significant drop in creep strain rate.

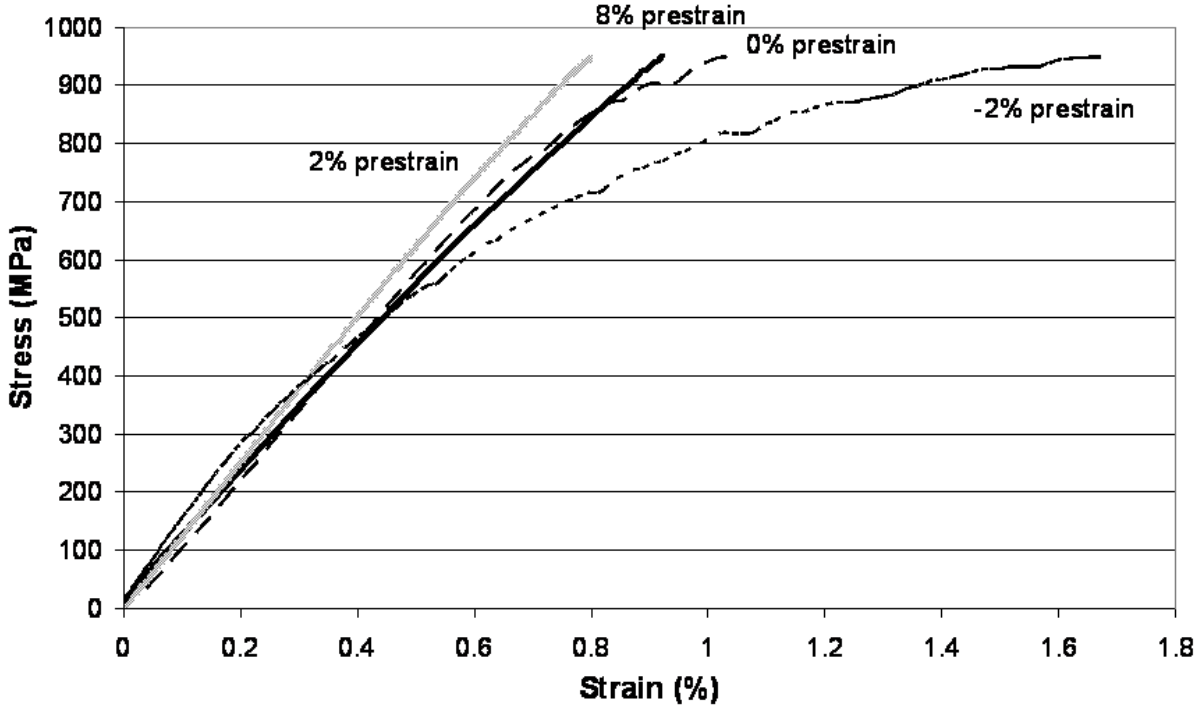

Figure 5: Loading curves for creep tests at 20°C. A lower yield stress occurs in the -2% specimen due to earlier yield in compression on prestraining. Strain hardening is clearly evident in the 2% and 8% specimens.

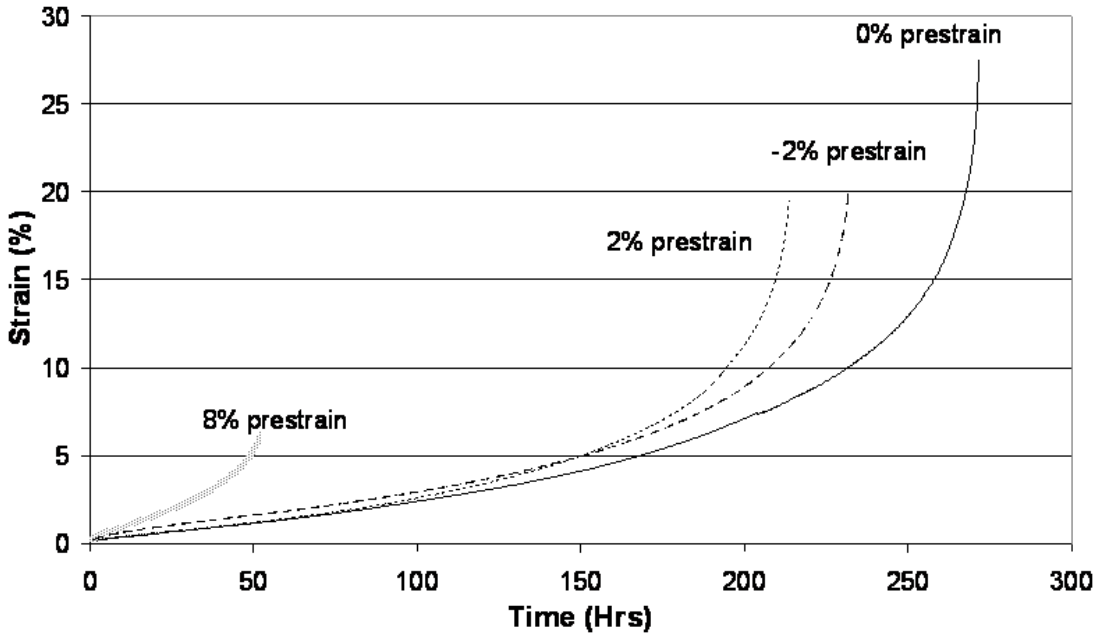

Figure 6: Creep curves at 600°C. at a stress of 400MPa It is clear that increases in prestrain level at this temperature cause a reduction in strain to failure and rupture time and an increase in creep strain rate.

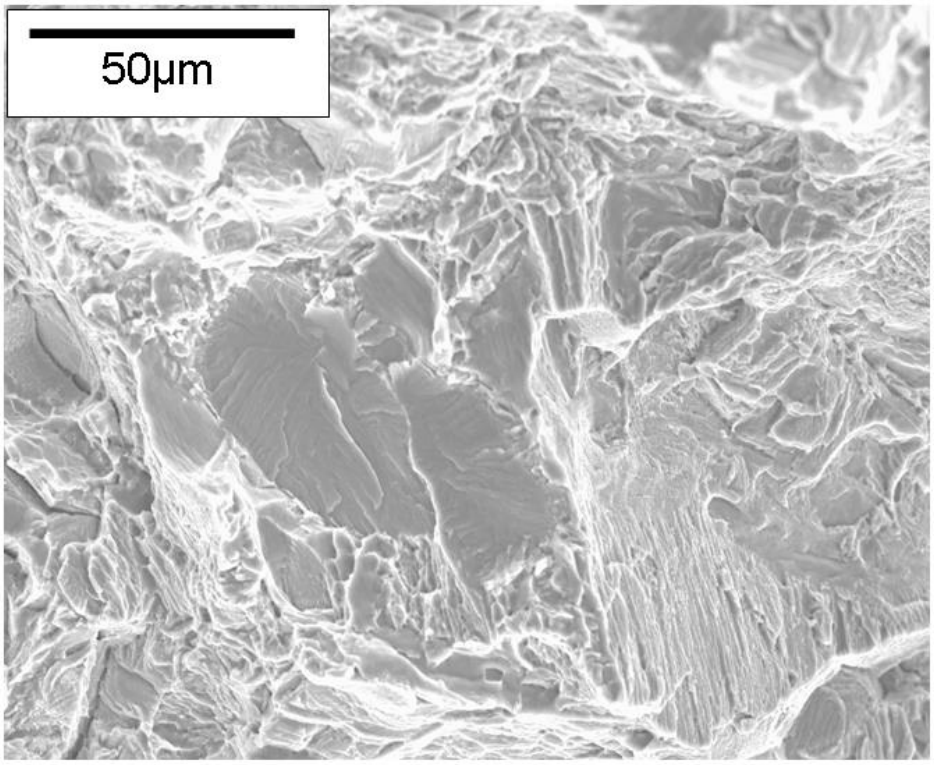

Figure 7: Isolated quasi-cleavage facet in 8% prestrain specimen. The facets do not form during the prestrain loading, but during a brief period of stress relaxation prior to unloading

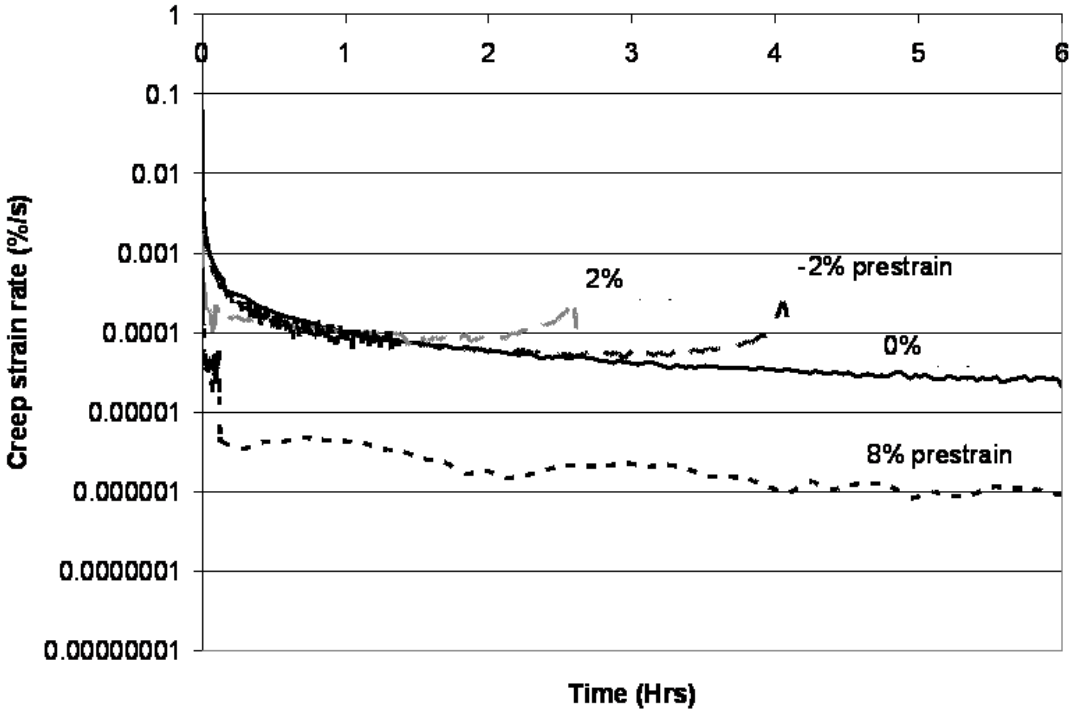

Figure 8: Creep strain rates in prestrained material. As would be expected during low temperature (logarithmic) creep a continuously decaying primary phase ends with a short accelerating tertiary phase and failure.

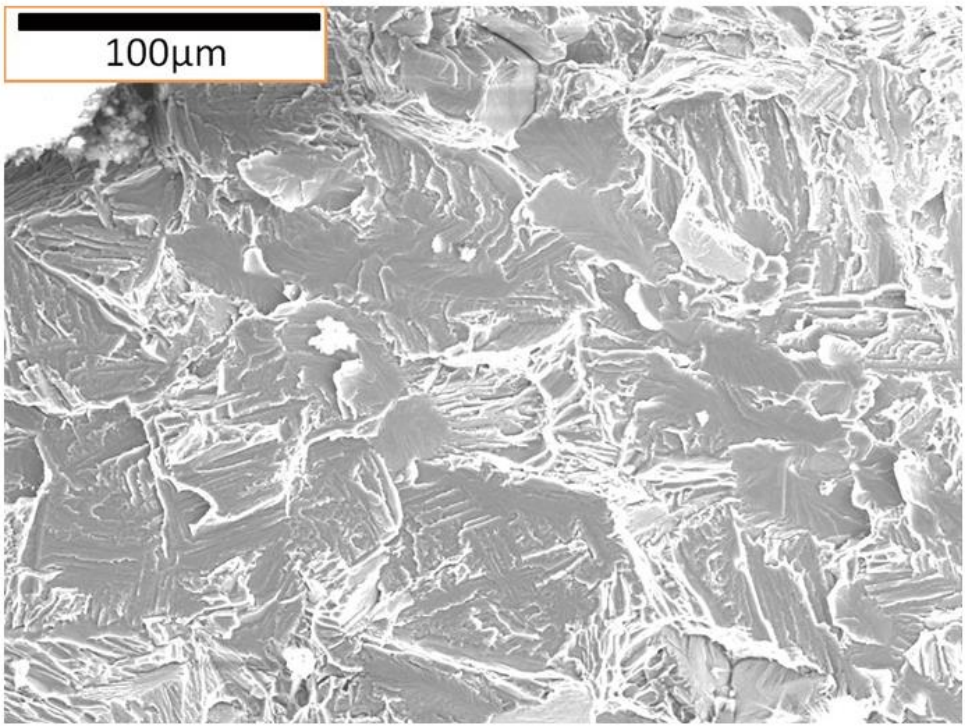

Figure 9: Faceted areas in cold creep specimen. The large amount of plasticity in these tests allows for cleavage on a large scale.

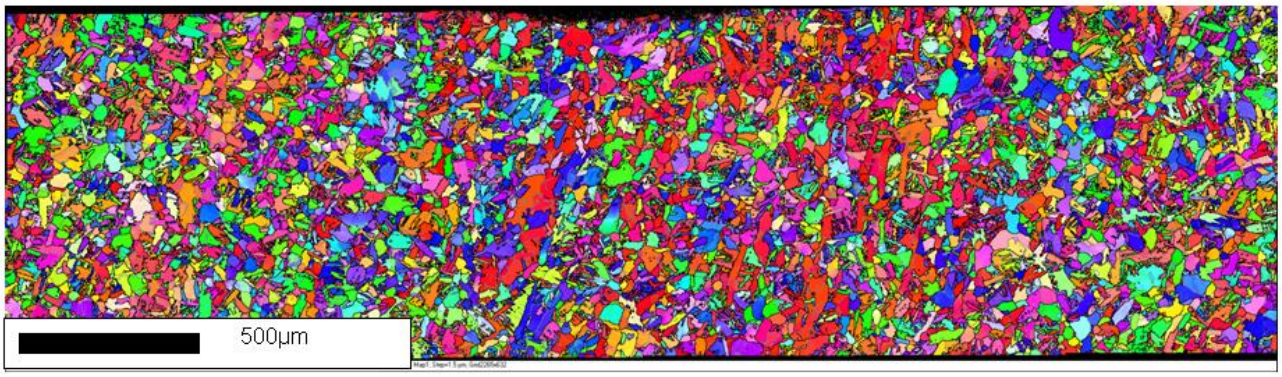

Figure 10: Crystal orientation map of Ti834 specimen indicating that no significant large areas of common orientation occur.

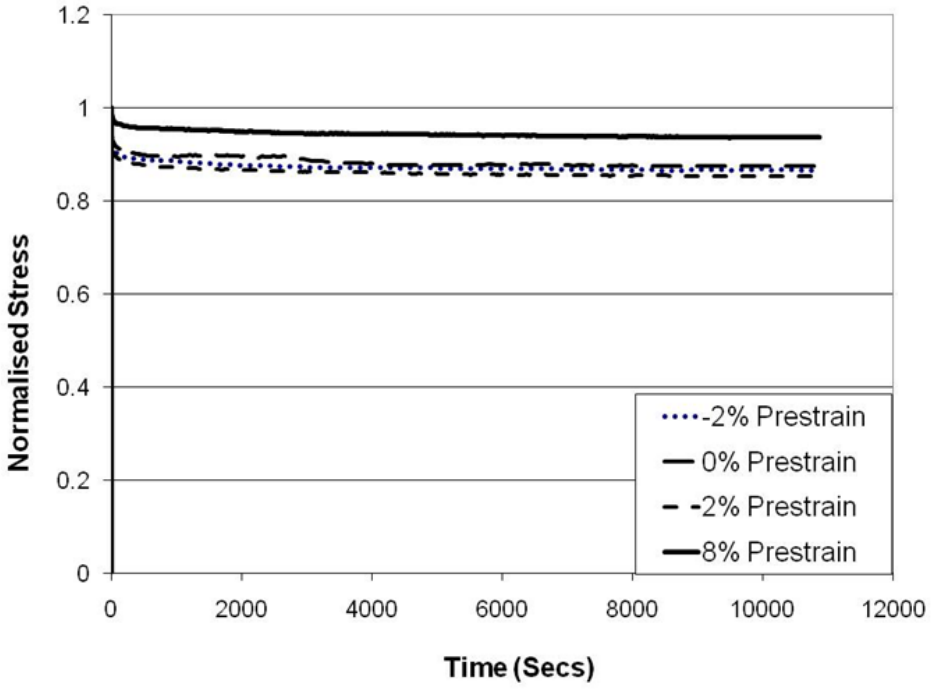

Figure 11: Stress relaxation of prestrained specimens, plotted as normalized stress, i.e. stress divided by peak stress achieved in that test. Significant differences are seen between the 8% prestrain specimen and other prestrain levels.

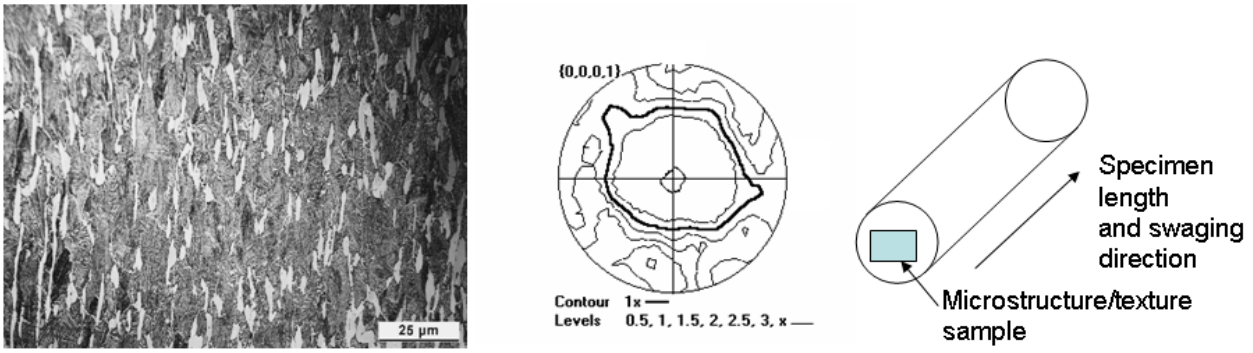

Figure 12: Microstructure and texture of Ti834 swaged material. The large amount of deformation is evident in the microstructure, and by the production of a well defined fibre texture. (Texture maps produced over an area of 0.5 x 0.5mm)

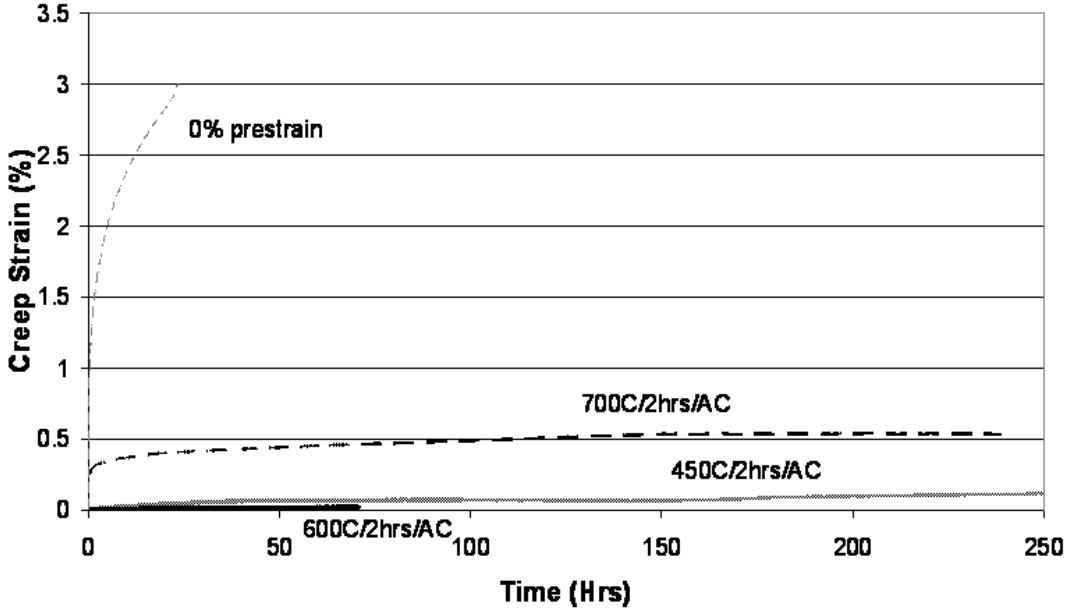

Figure 13: Creep curves for swaged material at 20°C indicating that heat treatments up to 700°C do not encourage significant recovery of dislocations, to allow low temperature creep.

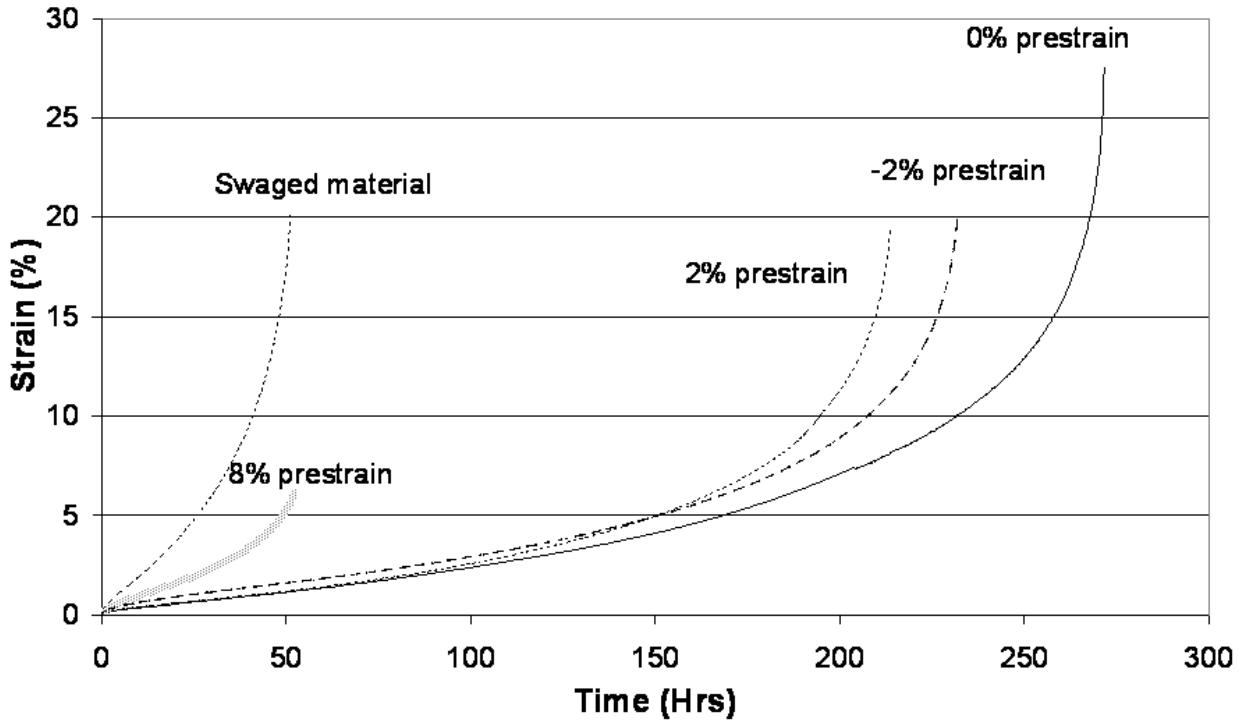

Figure 14: Creep curves at 600°C including swaged material. The swaged material follows the same trend as the prestrained material, in that higher deformation levels increase creep rate at these temperatures.

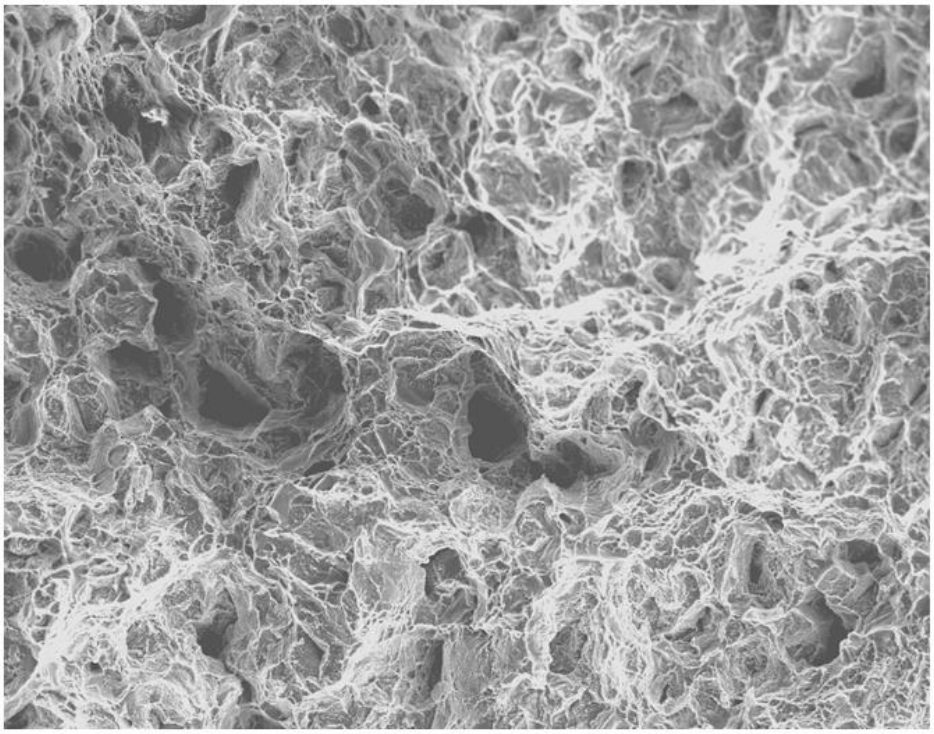

Figure 15: Ductile voids evident in Ti834 at 600°C. This type of feature is typical of high temperature creep phenomena.

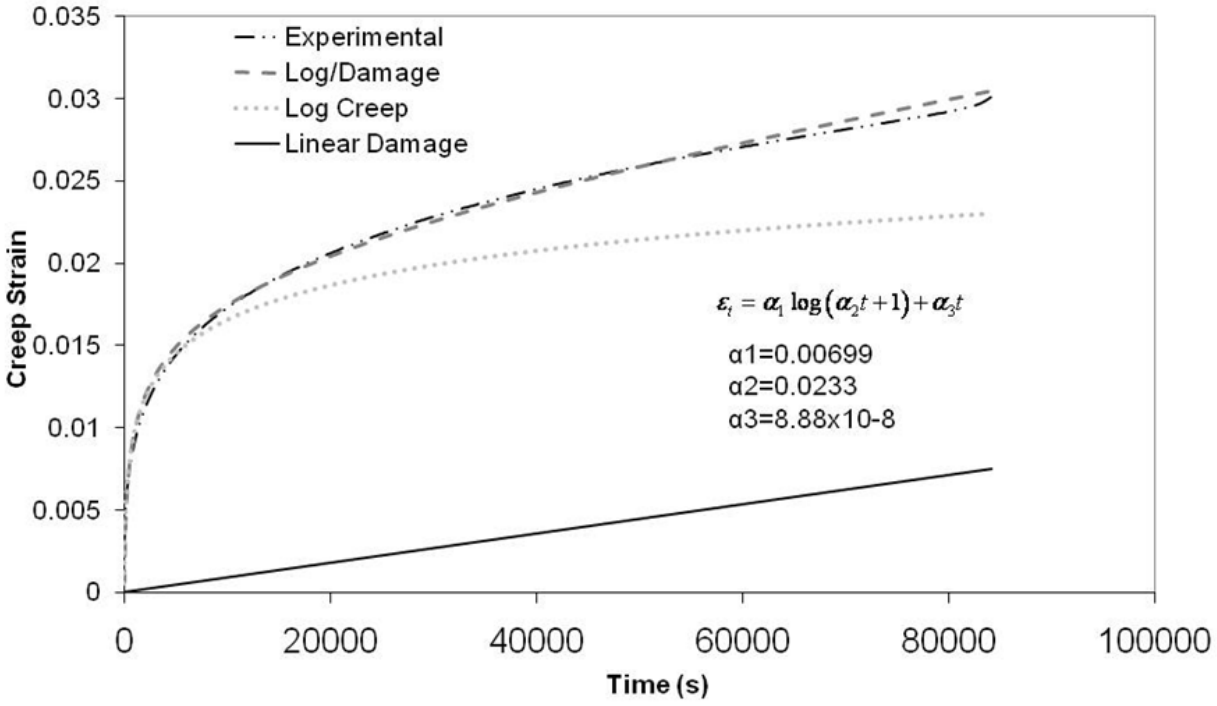

Figure 16: Modelling of cold creep in Ti834. It can be seen that an excellent representation of the curve is found by summing a logarithmic creep curve with a linear damage term.